

OPTICAL TIP-CLEARANCE PROBE FOR HARSH ENVIRONMENTS

Andreas Kempe, Stefan Schlamp, Thomas Rösgen

ETH Zürich, Institute of Fluid Dynamics, Sonneggstrasse 3, Zurich 8092, Switzerland

Ken Haffner

ALSTOM Power Switzerland

ABSTRACT

A measuring system based on low-coherence interferometry has been developed to obtain temporally resolved blade-by-blade tip-clearance data from the early stages of gas turbines. Given real-time tip clearance data, future turbines might be able to actively control the tip clearance by adjusting the amount of cooling air to the blades or shroud. Monitoring the tip clearance can also provide valuable information about the condition of the stage for maintenance. The measurement technique depends on the interference between back-reflected light from the blade tips during the blade passage time and a frequency-shifted reference. Due to the measurement principle the absolute spatial accuracy only relies on the coherence length of the light source. Normally this is a superluminescent diode with coherence lengths of tens of microns. For typical scenarios where the tip-clearances are within a range of a few millimeters, the technique can yield data once every second for each blade. This allows monitoring of transient effects during turbine start-up and shut-down. A single optical fiber of arbitrary length connects the self-contained optical and electronics setup to the turbine, thus separating it from heat, noise, and vibrations. The total cost of the optical probe is cheap enough so that the device can be made an integral part of a gas turbine for monitoring and it even allows for future active tip clearance control. The presented prototype of such a system is an all-fiber assembly, with self-calibrating capabilities and a spatial resolution of less than 50 μm . The data acquisition system consists of a digital storage oscilloscope and a common PC. The limited data transfer rates of this system lead to reduced scan rates (typically one per minute). Results from proof-of-principle measurements at different turbines, LISA test facility at ETH Zurich and GT26 gas turbine at ALSTOM, are reported in this paper.

INTRODUCTION

Leakage flows, i.e., fluid flowing through the gap between the blade tips and the casing of a turbine or compressor are responsible for a

significant percentage of the overall rotor losses and cause locally increased heat transfer rates (Sieverding 1989). Due to different thermal expansion coefficients and heating rates in the turbine rotor and the machine casing, the tip-clearance is not constant, but depends on the operation condition and varies during machine start-up and shut-down. In order to increase the turbine efficiency, the tip-clearance has to be as small as possible, while avoiding damage by blades touching the casing.

Current tip-clearance probes are mostly of inductive or capacitive type, with typical relative accuracies of about 5 % (Steiner 2000; Sheard et al. 1999). This is sufficient in situations where the probe can be mounted flush with the turbine casing, because the absolute errors are then small. In harsh and high-temperature environments, such as in the early stages of gas turbines, this mounting scheme is not feasible. The Curie point of rare earth metals, which is well below operating temperatures in turbines, sets an upper bound on the maximum operation temperature of these classical sensors (Dhadwal and Kurkov 1999; Barranger and Ford 1981). Innovative optical measurement probes can provide the required resolution and are generally not affected by temperature effects (Pfister et al. 2005).

The low-coherence interferometric tip-clearance probe presented yields near real-time blade-to-blade tip clearance data with absolute measurement errors in the order of tens of microns, even in harsh environments with limited optical access. The technique relies on interference between back-reflected light from the blade tips and a frequency-shifted reference. The low-coherence light source allows accuracies of better than 100 μm (typically 30 μm) independent of measurement distance, vibrations and temperature changes. Optical access is provided by a single optical fiber of arbitrary length. The robust sensor head can easily be mounted in a cooled recess. Its maximum operating temperature is ~ 1000 K. The sensitive mechanical, electronic, and optical components of the system are placed far from the turbine in a separate post-processing unit.

MEASUREMENT PRINCIPLE

Fig.1 shows the schematic setup of the optical components in the measuring circuit of the system. A superluminescent diode (SLD, Superlum Diodes Model SLD56-HP2, 10 mW) emits low-coherence light into a single-mode fiber. A fiber-optical isolator protects the sensitive light source from back reflections and guides the light to a polarization-insensitive optical circulator. The circulator is used to transfer the light through a single-mode optical fiber to the endoscopic front end (EFE), where a collimator lens directs the light out of the fiber onto the passing blade tips. A small fraction of the incident light is reflected back onto the collimator lens and into the fiber towards the circulator, where it is deflected into the interferometer part of the measurement system. A small fraction ($\sim 1\%$) of the light is also reflected off the two surfaces of the collimator lens, which provides a spatial reference. Following the nomenclature of Fig. 2, the light reflected from the blade tips is denoted as ray 1 and the light reflected from the lens's front and back surfaces as rays 2 and 3, respectively. The light back-reflected from the turbine blades and the collimator surfaces (rays 1, 2, 3) is fed into two interferometer arms by a beam splitter. In the reference arm, an acousto-optical modulator (AOM, NEOS Model 26055) shifts the frequency of the light by 55 MHz, corresponding to several periods within the blade passage time ($\sim 1\ \mu\text{s}$). The delay arm contains a motorized variable delay line (VDL, General Photonics VariDelay). The light from the two interferometer arms is re-combined by another beam splitter/combiner and a broadband photo-receiver (New Focus Model 1811) serves as detector.

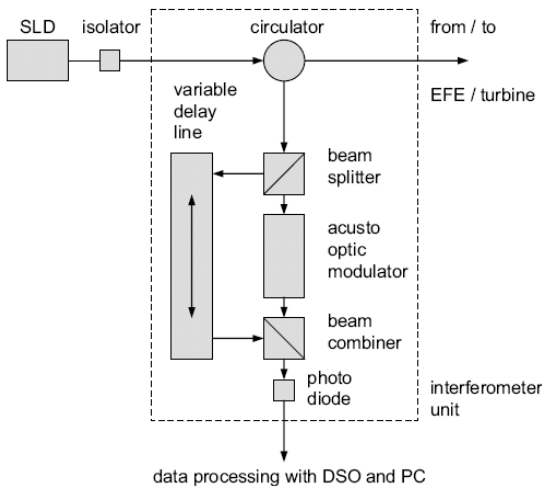


Figure 2: Schematic setup of optical components in the interferometer unit, which also includes the light source.

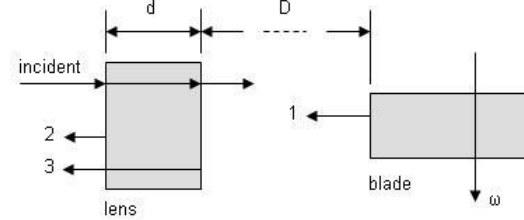


Figure 1: Incident light and sources of reflections.

As shown in Fig. 2, the path length of ray 1 is longer than that of rays 2 and 3. Denote the tip-clearance as D , the optical thickness of the collimator lens as d and the path lengths of both interferometer arms (between the two beam splitters/combiners) as l_{ref} and l_{delay} , respectively. If the VDL is set such that $l_{\text{ref}} + 2(D+d) = l_{\text{delay}}$, for example, the part of ray 1 going through the reference arm interferes with those parts of ray 2 which go through the delay arm. The frequency of the AOM is now recorded as a beat-signal at the detector, which is detected as a peak in the power spectrum. Similarly, interference between ray 1 and ray 3 is observed, when $l_{\text{ref}} + 2D = l_{\text{delay}}$. By checking the delay setting where ray 2 and ray 3 interfere, i.e., when $l_{\text{ref}} + 2d = l_{\text{delay}}$, the system can be calibrated with the known thickness and thermal behavior of the sapphire lens used in the custom made EFE.

SIGNAL PROCESSING

Fig. 3 shows the data acquisition chain used for the experiments in this paper. The analog signals from the photo-receiver are first filtered by a bandpass-filter (Mini Circuits BIF-60) and then amplified by 36 dB with a high speed amplifier (Hamamatsu C5594-12). The reconditioned signals are then digitized with 8.Bit precision by a Digital Storage Oscilloscope DSO (LeCroy LT347L). Data is then transferred to a PC through a 10.MBit Ethernet connection for further analysis and storage. The sampling rate and the acquisition window length are set through the DSO. The DAQ is initiated by triggering the DSO with an external key-phaser of the test facility.

Two LabView (Ver. 7.1, National Instruments) programs perform the data storage and analysis. While one of them only stores the raw data for later analysis, the second extracts tip clearances either on-line or from previously stored data sets. During the critical gas turbine tests, data was initially only stored. The raw data is first bandpass filtered with a second-order Butterworth IIR-filter with a

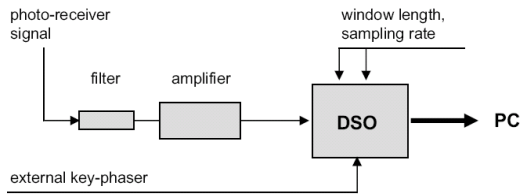


Figure 3: Data acquisition chain for Tip-Clearance experiments.

frequency range of 55 ± 1 MHz. A reliable indicator of a blade passage at the current delay line setting was found to be the product of the signal variance and the maximum of the power spectrum within a few microseconds sliding window. Either one of these factors on its own did not yield satisfactory discrimination between blade passages and noise, especially at low signal levels. This product will be referred as beat signal intensity for the remainder of the paper.

Suppose that data is acquired for the entire duration of a turbine revolution. The VDL delay is varied in steps after each acquisition and a new full-revolution trace is acquired. The step size for the VDL has to be less than the coherence length of the light source. This, combined with the given rotation rate of the turbine and the desired measurement range, is an upper bound for the detection rate of the technique. A full scan over 1 mm in steps of $40 \mu\text{m}$ on a turbine operating at 50 Hz thus requires at least 1 s. Note that data acquisition and moving the VDL occurs during alternating revolutions. In practice, achievable data transfer rates and the response time of the VDL motor led to increased scan times.

Two approaches to reduce the amount of raw data were used. One is undersampling of the DSO at sampling rates of 50, 20 and 10 MHz. The Butterworth filter then had a frequency range of 5 ± 1 MHz. Noise from multiple frequency ranges is convolved into the relevant frequency range. This leads to reduced signal-to-noise ratios (SNR). For tests in turbines, however, it was found to be acceptable. A further reduction of the amount of data can be realized by only acquiring data within short windows around the expected blade passage time. For turbine stages with many blades and using window sizes which capture the blade passage reliably, however, the benefits are small. If the SNR is low, averaging over several revolutions can be employed. Averaging is then performed over the beat signal intensities.

The signal analysis produces a two-dimensional map of the beat signal intensity, i.e., intensity vs. delay line setting and time within each revolution. An example is shown in Fig. 5. A large value of the beat signal intensity indicates that a blade passage at the set path length difference has

been detected. The vertical length of the lines depends on the coherence length of the light source and the step size of the VDL.

RESULTS

LISA test turbine

LISA (see Fig. 4) is a research turbine test facility of the Laboratory of Turbomachinery at ETH Zurich. The important design features are mechanical precision, full accessibility for instrumentation as well as quick assembly. The core of the test stand is an axial turbine with vertical orientation. The maximum power of 400 kW is taken from a quasi atmospheric air circuit driven by a 750 kW radial compressor. The turbine's power output is connected via an angular gear box to a generator with electrical power feedback. The air circuit consists of a cooler, which controls the inlet temperature, a flow conditioning segment and a calibrated venturinozzle integrated into the back flow pipe (LSM 2006). The results of

LISA tip-clearance tests presented in this paper were performed as a piggyback experiment during tip gap flow field manipulations (Behr 2006).

Due to the high mechanical precision of the turbine as well as the use of cold gas (approx. 50°C) and therefore small thermal expansion responses, the focus of the measurements was to scan with high spatial resolution, i.e., small interferometer delay steps. Fig. 5 shows a two-dimensional intensity map over 50 milliseconds at a rotation speed of 2700 rpm, i.e., spanning two full revolutions. The sampling rate was set to 50 MHz, the step size to $20 \mu\text{m}$. The whole scan over 0.3 mm lasted 60 seconds. The rotor with a tip diameter of $798.6 \text{ mm} [\pm 0.01 \text{ mm}]$ consists of 54 blades machined into one single aluminum ring by electrical erosion. The smooth aluminum surface of

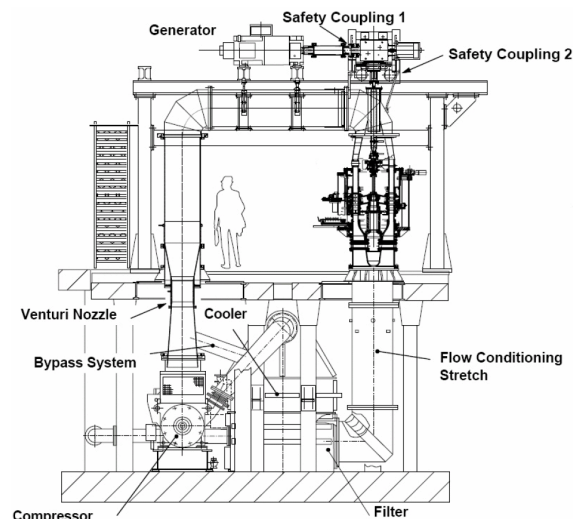
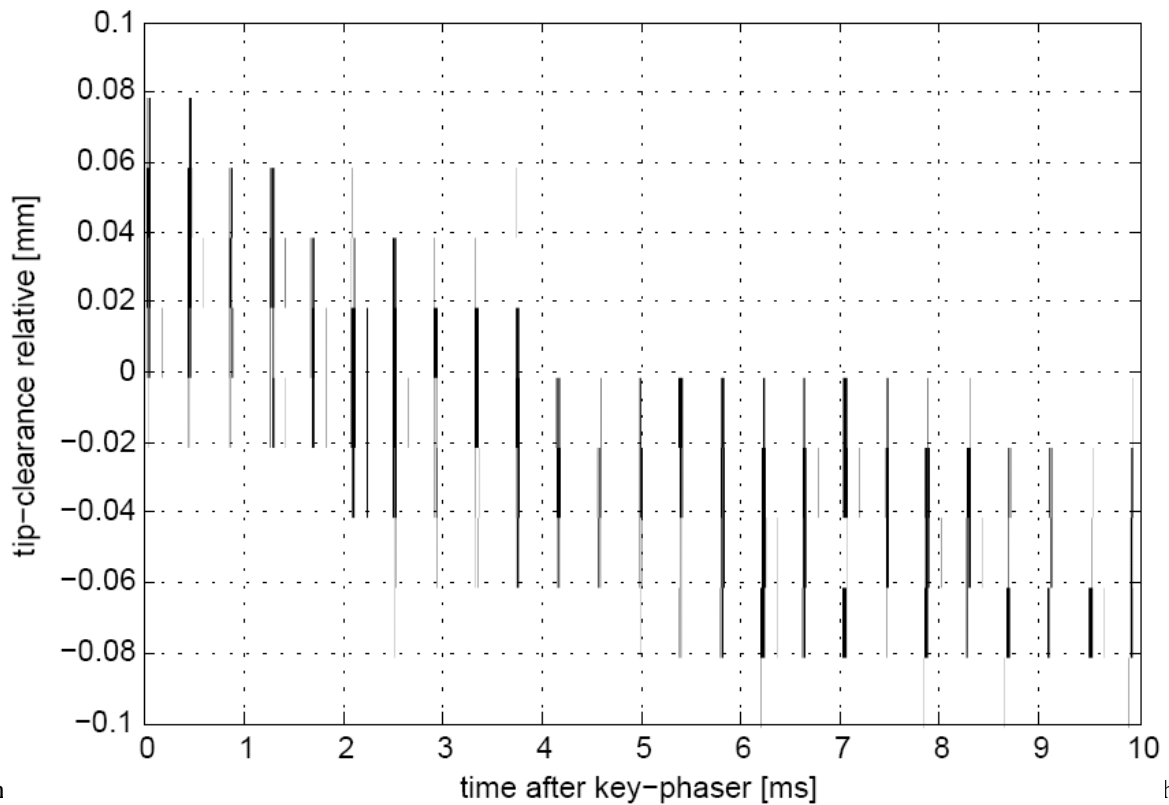
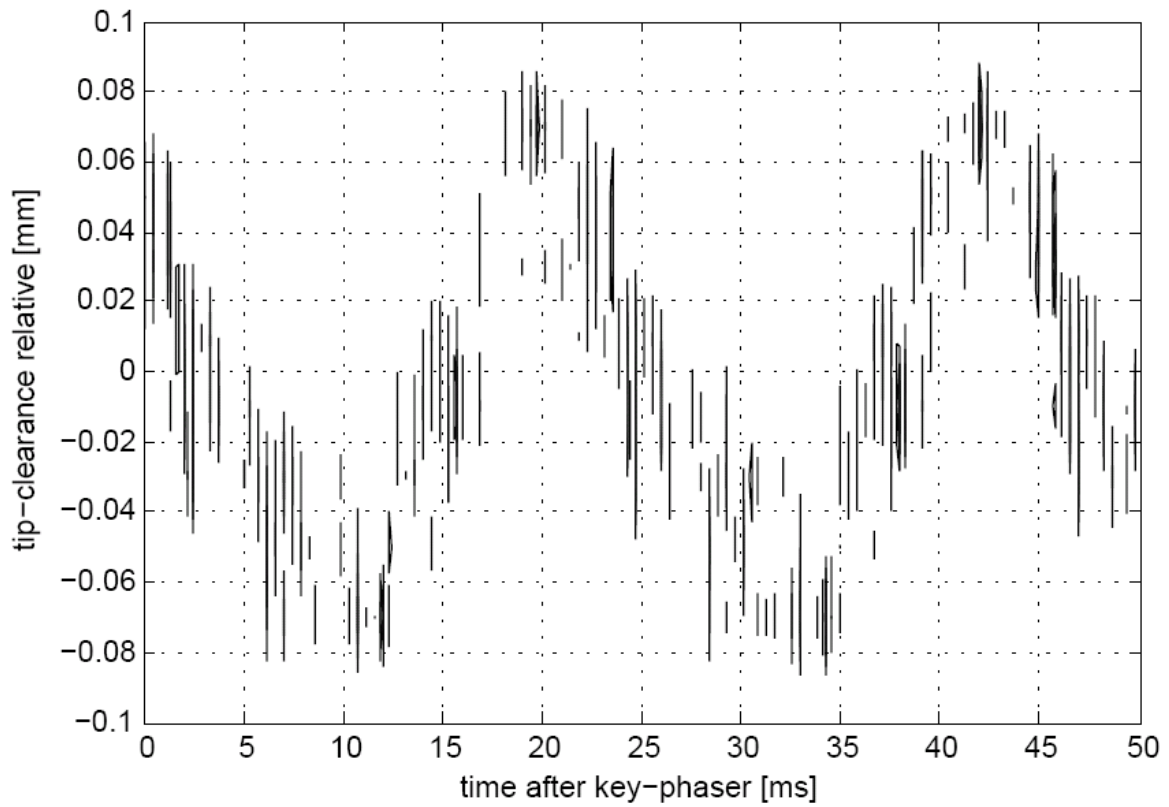


Figure 4: LISA test facility, Laboratory of Turbomachinery at ETH Zurich.



th Together with the signal amplification due to the interference with the reference reflection in the EFE, the SNR in these tests is not a critical issue.

The rotor blade tips show a sinusoidal clearance behavior with an amplitude of approx. 50 μm . This value might be due to a small

the turbine. In Fig. 6 the average, the maximum and the minimum tip-clearance of the 54 blades was recorded over time. The sampling rate was 10 MHz and the step size 20 μm . In this test, a separate spatial reference was provided by a window which was placed approximately flush with the casing.

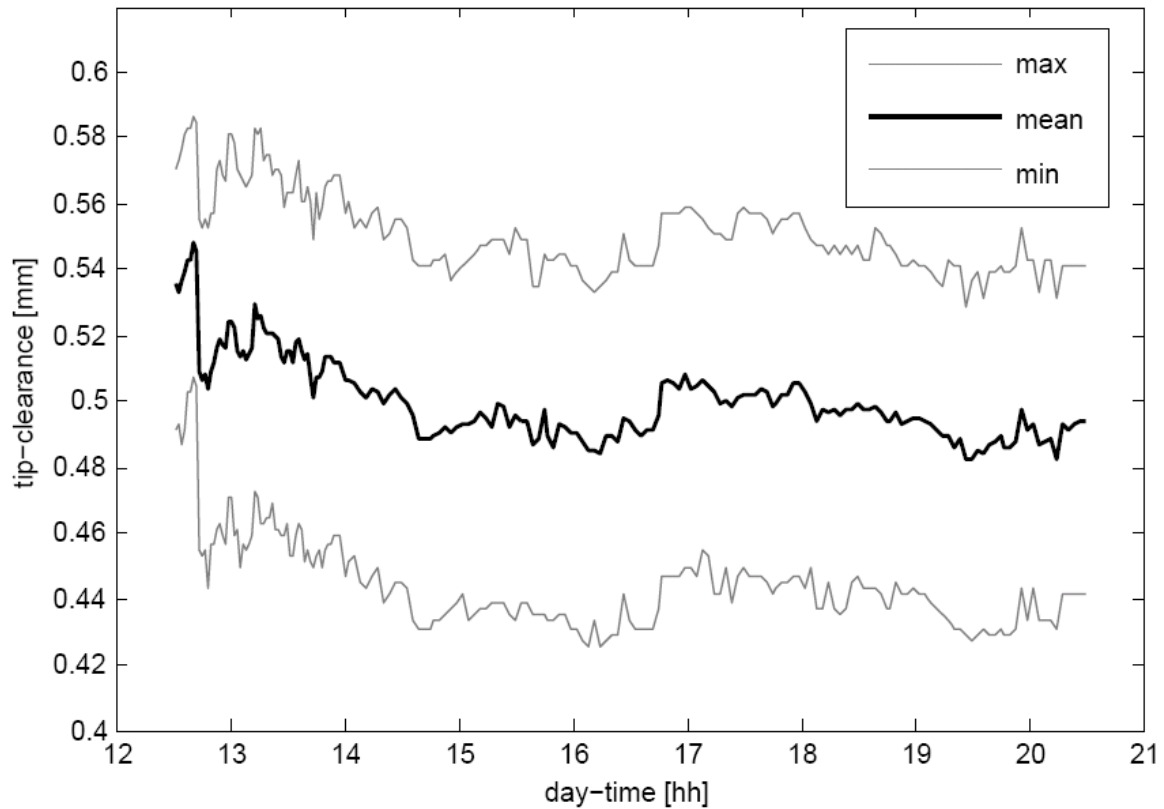


Figure 5: Intensity map of LISA test a.) 50 ms b.) zoom in 10 ms

The scan range was increased to 1.15 mm so as to include this reference location. The EFE itself was at a distance of approx. 3 cm from the blade tips due to its design for the GT26 tests. A scan then lasted 95 seconds. The long-term clearance behavior of the turbine shows a small decrease of the gap by about 100 μm (before 13 hours daytime, the turbine was rotating at a lower speed). Additionally a smooth increase and decrease of the tip-clearance can be detected. This might be due to a slow, gradual rotation of 20° of the turbine casing during the simultaneously performed flow field measurements. However it must be noted that the clearance changes are almost within the measurement accuracy of the system.

GT26 gas turbine

The GT26 gas turbine is specifically developed for combined cycle applications. It is designed to burn natural gas as a primary fuel and diesel as backup fuel. In terms of operational flexibility, the GT26 can be found operating in all three major modes: base load, intermediate duty and daily start and stop. At 50 Hz rotation speed and in combined cycle the GT26 has approx. 281 MW electrical output (about 260 MW are directly related to the gas turbine). Its smaller counterpart is the GT24 with approx. 188 MW electrical power. The GT24 / GT26 are provided with a sequential combustion

system consisting of an environmental (EV) and a sequential combustor (SEV). The sequential combustion system is unique to the ALSTOM GT24 /GT26 gas turbine type and applies the thermodynamic reheat principle (ALSTOM 2006).

The tests at GT26 were primarily performed to demonstrate the performance of the measurement system under operational conditions, i.e., high temperatures and weak reflection levels from the coated turbine blades, as well as the short passage time of the blades (approx. 10 μs). Tests were performed at the first stage behind each combustor under the major operation modes, with gas or oil as fuel. Due to confidentiality aspects, the results of these tests cannot be illustrated in this paper. In general it can be said that also under real gas turbine conditions, the sensor still works well. Similar to the LISA experiment, the tip-clearance for each blade in a stage could be measured. The measuring rate was high enough to monitor the transient effects during the engine start-up.

Fig. 6.4, as an example, shows only a part of an intensity plot (note: the absolute tip-clearance values have been changed). The delay step value was set to 40 microns, which in turn is the measurement accuracy. Larger step values are not possible, due to the coherence length the light source of approx. 50 μm . The time axis is resolved with 5 microseconds. The signatures show that the

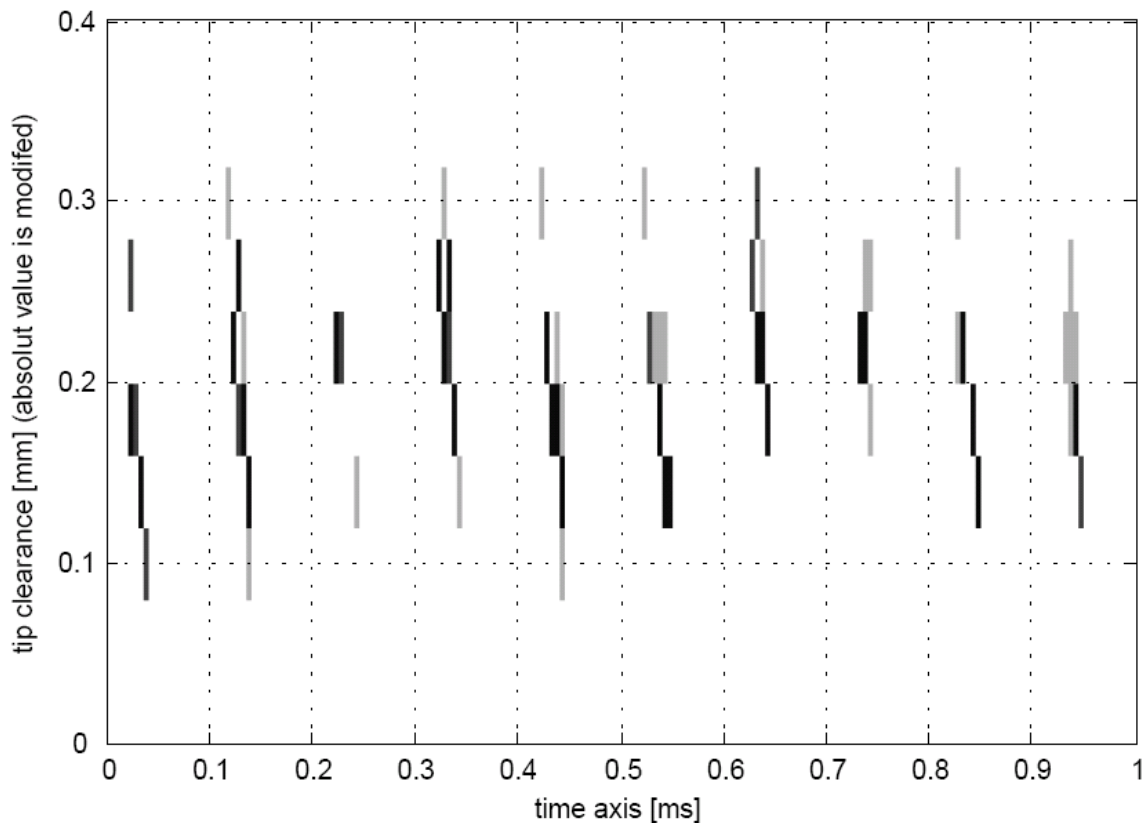


Figure 5: Intensity map of LISA test a.) 50 ms b.) zoom in 10 ms

blade tip is not flat, but slightly beveled. However, in terms of measurement system performance a couple points need to be pointed out.

The EFE with its optical parts close to the hot gas flow showed no irreversible failures. The high temperatures and the mechanical loads due to the casing movements during its warm-up did not damage the optics. The 20 m fiber optical extension cable could also withstand the temperatures within the turbine enclosure, which can reach up to approx. 80°C close to the turbine.

The SNR was high enough to operate with a sampling rate of 50 MHz and without averaging. During the start-up of the turbine, i.e., the first 30 minutes after ignition, the SNR was comparatively low and just above the sensing limit. Furthermore, after 5 hours of operation under base load conditions, the SNR dropped over a period of 20-30 minutes. Finally and reproducibly in two tests at around 5-6 hours of operation, the SNR was too low to detect any tip-clearances. Both phenomena are probably caused by changes in the thermal behavior of the optical fibers within the casing and the turbine enclosure. The first decrease of the SNR at the start-up might be due to the fast temperature rise and therefore the huge thermal stresses at the EFE. After 30 minutes, the rate of the temperature rise decreases. The whole EFE is heated-up and due to its design the fiber within the

EFE experiences no mechanical stresses. The second decrease can be attributed to the relatively small thermal load in the turbine enclosure. The extension cable was protected by a thick PVC tube (standard telecom cable). Its thermal insulation might cause the long response time to the temperatures in the enclosure building. The assembly of the fiber and the PVC are not specially designed to balance mechanical stresses of the fiber at higher temperatures. In that way, under stress the fiber transmissivity can drop by orders of magnitude. However, both assumptions theories must yet be investigated in further tests.

During the GT26 tests the beat signal frequency was shifted by 10 to 15 MHz. This is due to Doppler effects in the back-reflected light from the blade tips. If the surface of the blade tips moves not perpendicularly to the sensor head, a Doppler shift can be detected as in common LDA applications. In this scenario only a single beam is necessary. Any relative velocities parallel to the beam axis between the reference reflection and the blade reflection will result in a Doppler signal. In the GT26 the blade tips are relatively rough, plus they are slightly beveled. The roughness leads to a spectral broadening of the beat-signal frequency of up to ± 2 MHz. The bevel of the tip causes a general frequency shift. It might also be possible that the sensor was mounted at a small angle.

Taking into account the circumferential velocities at the GT26 of approx. 370 m/s, the observed frequency-shift corresponds to an angle of about 1° - 2° off the normal direction. In the data acquisition and analysis this Doppler shift has to be considered. All bandpass filter devices have to match the shifted frequency. For industrial applications such uncertainties in the analysis regime are not desirable.

CONCLUSIONS

Proof-of-principle measurements were presented for a novel tip-clearance measurement technique with high spatial and temporal resolution. Independent of the distance between the output coupler lens and the blade tip the absolute spatial accuracy is better than 50 microns. Variations in fluid or material temperatures have no influence other than minimal changes in the refractive index. Data acquisition rates for tip-clearances in the order of seconds allow monitoring of transient effects during turbine start-up and shut-down. Simultaneously to the tip clearance, the blade passage times are measured, allowing one to detect blade oscillations.

The tests at the LISA turbine test facility and the GT26 gas turbine under operational conditions already led to satisfactory results. However, for a second prototype the aspect of industrial operation have to be considered. One focus is the thermal behavior of the optical fibers close to the turbine. In particular the problem in long-term tests has to be solved. An exposure of the optical connection cable to an environment of 80°C leads to a reversible failure after approx. 5 hours. With special assemblies the optical fiber in the covering tube can be guided stress-free, which should solve this problem. The second focus lies in the observed Doppler effects which lead to a shifted beat signal. A new interferometer setup without acousto-optic modulator, but with direct SLD amplitude modulation will make the system insensitive to Doppler shifts in the light received from the blade tips and is much simpler. Both of these aspects are currently under further investigation.

ACKNOWLEDGEMENTS

This work was funded by ALSTOM Power Switzerland as part of the Center for Energy Conversion (CEC) initiative.

REFERENCES

- ALSTOM (2006) GT24 and GT26 Gas Turbines - 188MW and 281MW. www.power.alstom.com (last visited 15.05.2006)
- Barranger JP, Ford MJ (1981) Laser Optical Blade Tip Clearance Measurement System. *J Eng Power* 103(2):457-460
- Behr T, Kalfas AI, Abhari RS (2006) Unsteady Flow Physics and Performance of a One-and-1/2-Stage Unshrouded High Work Turbine, SME Paper No. GT2006-90959
- Dhadwal HS, Kurkov AP (1999) Dual-laser probe measurement of blade-tip clearance. *J Turbomach* 121:481-485
- Heard AG, O'Donnell SG, Stringfellow FF (1999) High temperature proximity measurement in aero and industrial turbomachinery. *J Eng Gas Turbines Power* 121:167-173
- LSM (2006) LISA Axial Turbine Test facility. <http://www.lsm.ethz.ch> (last visited 15.05.2006)
- Pfister T, Büttner L and Czarske J (2005) Laser Doppler profile sensor with sub-micrometre position resolution for velocity and absolute radius measurements of rotating objects. *Meas Sci Technol* 16:627-641
- Sieverding C (1989) Tip-Clearance Effects in Axial Turbomachines. Lecture series 1985-5 (Von Karman Institute, Rhode-St-Genese)
- Steiner A (2000) Techniques for blade tip clearance measurements with capacitive probes. *Meas Sci Technol* 11:865-869